

Full paper

Sit-to-Stand and Stand-to-Sit Transfer Support for Complete Paraplegic Patients with Robot Suit HAL

Atsushi Tsukahara*, Ryota Kawanishi, Yasuhisa Hasegawa and Yoshiyuki Sankai

Systems and Information Engineering, University of Tsukuba, 1-1-1 Tennodai, Tsukuba, Ibaraki 305-8573, Japan

Received 11 September 2009; accepted 19 November 2009

Abstract

Physical support of lower limbs during sit-to-stand and stand-to-sit transfers is important for an independent life of paraplegic patients. The purpose of this study is, therefore, to realize the control method of complete paraplegic patients during sit-to-stand and stand-to-sit transfers by using a ‘robot suit HAL’. It is the most challenging issue because the HAL should start supporting the wearer’s motions synchronizing his/her intention. Our proposed algorithm infers the intention based on a preliminary motion that is observed just before a desired motion so the patient could start the sit-to-stand or stand-to-sit transfers without any operation. When the HAL detects the intention to stand up and sit down, the HAL starts to support the wearer’s weight and to control their body posture for stability during their transfer. The proposed algorithms embedded in the HAL were applied to a complete spinal cord injury patient in a clinical trial to confirm the effectiveness. The experimental results indicate that the proposed algorithms could support his sit-to-stand and stand-to-sit transfers safely and conveniently by keeping his stability and by reflecting his intentions. Consequently, we confirmed that the proposed method successfully supported the sit-to-stand and stand-to-sit transfers of the complete paraplegic patient with the HAL.

© Koninklijke Brill NV, Leiden and The Robotics Society of Japan, 2010

Keywords

Robot suit, complete paraplegic patients, sit-to-stand, stand-to-sit, motion support

1. Introduction

Generally speaking, medical doctors and physical therapists emphasize sit-to-stand training and stand-to-sit training for rehabilitation of paraplegic patients who have an impairment in their legs due to spinal cord injury (SCI), cerebrovascular accident, etc. That is the reason why the training brings several advantages such as expansion of the range of motion, activation of the circulatory and respiratory

* To whom correspondence should be addressed. E-mail: tsukahara@golem.kz.tsukuba.ac.jp

systems, alleviation of spasticity, and prevention of scoliosis. Training of the sit-to-stand transfer using long leg braces increases the bone mineral density at the proximal femur to a remarkable degree [1]. Daily training also prevents side-effects such as orthostatic hypotension, osteoporosis and bedsores. However, if patients received the spinal cord surgery due to a traffic accident, a spinal cord infarction, etc., they cannot sufficiently move their legs after the surgery. It is essential for the patients to undergo such training soon after the surgery so as to recover deteriorating motor and sensor functions of their legs.

An exoskeletal assistive system ‘robot suit HAL (Hybrid Assistive Limb)’ shown in Fig. 1 has been developed to physically support the patient as well as a healthy person [2–5]. As a result, the patient easily starts rehabilitation at the beginning of the recovery phase, and the physical therapist is also relieved from assistance of weight and leg motion of the patient. In order to support various types of people, from a healthy person to a completely paraplegic patient, we have also designed control algorithms specialized to wearers. One of the algorithms, i.e., ‘cybernic voluntary control’, controls the actuator torque of HAL to augment joint torque of the wearer according to the voluntary muscle activity that is estimated from the bioelectrical signals (BESs). The BES including myoelectricity is useful and reliable information to synchronize a motion support with the wearer’s motion because the BES is measured just before the corresponding muscle activities. Additionally, HAL also has another control algorithm, i.e., ‘cybernic autonomous control’, that supports a functional motion that is desired by the wearer. The wearer’s intention related to the desired motion is inferred from a preliminary motion that he/she takes just before the desired motion, because the proper BES is not measurable from the

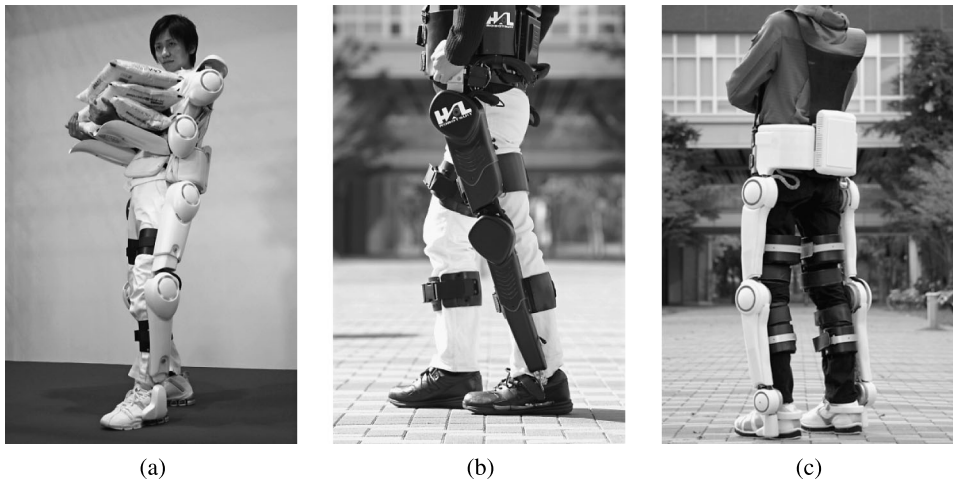


Figure 1. Representative conventional robot suit HAL-5 developed to expand and improve physical capabilities of a human being. This study uses the latest HAL-5 LB ‘Type-C’. The power units are attached to each joint. (a) HAL-5. (b) HAL-5 LB ‘Type-B’. (c) HAL-5 LB ‘Type-C’.

lower limbs of severely compromised patients. This approach is one of the ideal solutions to support the lower limbs of a severely compromised patient, because the patient wearing the HAL is assisted in his/her functional motion by using the wearer's residual function for the preliminary motion. This cybernic autonomous control is applied to the functional training of lower limbs soon after the surgery. Depending on the patient's condition, some part of the wearer's body can be supported by the cybernic voluntary control, while the other part can be supported by the cybernic autonomous control. For example, the number of joints supported by the cybernic voluntary control is gradually increased according to the patient's recovery phase. This paper focuses on the functional motion support for complete paraplegic patients. Only cybernic autonomous control is, therefore, used in this paper. The main contributions of this paper are a mechanical design and control algorithms of the support system for complete paraplegic patients during sit-to-stand and stand-to-sit transfers.

Meanwhile, several devices for sit-to-stand and stand-to-sit transfer support have been developed [6–14]. These devices share the patient's weight with the wearer's legs and decrease the knee joint torque of the wearer when their knee joints are bending. It is better for elderly persons or complete paraplegic patients to use their legs to support their weight due to the various reasons explained above. However, one of the limitations in these studies is that it does not contribute to the wearer's posture control due to a lack of degrees of freedom. The posture control is also indispensable to stand up and sit down for safety and stability. In addition, it is difficult to support sit-to-stand and stand-to-sit transfers that are synchronized with the patient's intention. If the HAL can safely support the sit-to-stand and stand-to-sit transfers of complete paraplegic patients synchronizing the wearer's intention, it can promote the independent life of physically challenged persons to a further advanced stage.

In this paper, we propose algorithms to support the wearer's weight and to control the wearer's body posture for stability during the sit-to-stand and stand-to-sit transfers, i.e., a gravity compensation algorithm and a balance control algorithm. The balance control algorithm controls the wearer's center of pressure (COP) for stability. The gravity compensation algorithm supports the wearer's weight so as to lower the error from the reference angles, if a constant large force such as gravity affects the joints of the HAL. These algorithms generate the torque of each joint of the HAL. The HAL used in this study simultaneously assists the functional motions of lower limbs with the multiple joints, using power units attached on the hip, knee and ankle joints. In addition, a useful interface is also desired to directly convey the wearer's intention with regard to the start of the desired motion to the assistive device, such as a brain–computer interface. The BES is a kind of information to infer the wearer's intention related to his/her motion. Unfortunately, the proper signals cannot be observed from patients such as complete SCI patients. This paper, therefore, proposes an intention estimation algorithm for the HAL to start sit-to-stand and stand-to-sit transfer support based on a preliminary motion of their upper body

and posture condition. This preliminary motion can normally be observed immediately before the desired motion.

The purpose of this study is to realize the control method of complete paraplegic patients during sit-to-stand and stand-to-sit transfers by using the HAL. The 'HAL-5 LB (Type-C)' supports the functional motions of the lower limbs with multiple joints actuated by power units.

2. Robot Suit HAL

The HAL-5 LB 'Type-C' is developed to support the various lower limb functions of physically challenged persons with different physiques. The configurations are shown in Fig. 2. The HAL consists of power units, exoskeletal frames, sensors and a controller. Exoskeletal frames are fixed to the wearer's legs with molded fastening equipment. Potentiometers are attached to each joint to measure the relative angles. A triaxial accelerometer is located in a control box to measure absolute angles of a wearer's trunk. The HAL can calculate the wearer's COP precisely by using the floor reaction force (FRF) sensors (Fig. 3a). These sensors utilize semiconductor-type pressure sensors and are installed in the shoes. The weight of the HAL and the wearer is measured by the pressure of inner bags embedded in a plantar part of the shoes. A computer and batteries are attached on the wearer's waist, and motor drivers and other electrical circuits are allocated on each power unit. Power units are directly attached on each joint of the HAL. The actuator torque is transmitted from the HAL to the wearer's limbs through the molded fastening equipment.

It is necessary to firmly sustain a standing posture during sit-to-stand and stand-to-sit transfers support for a patient with severe dysfunction such as a complete paraplegic patient. In this study, an anti-flexion bar has been developed to prevent misalignment of the knee joints of the patient and the HAL. Figure 3b shows a lower thigh frame of the HAL-5 LB 'Type-C' equipped with the anti-flexion bar. It holds a wearer's leg on the patella tendon between the patella and the upper end of the tibia so as not to directly compress bones and nerves, so that the bar could prevent a wearer's knee joints from going forward while standing.

A knee joint needs high torque in an extension direction during a sit-to-stand transfer because the knee joint lifts up the center of gravity (COG) of the wearer. However, a knee joint does not need high torque in a flexion direction during a stand-to-sit transfer. Therefore, a tension coil spring is installed in knee joints of the HAL to support only extension torque of the knee joint. The passive device is also effective to miniaturize a power unit and to decrease energy consumption. The coil spring, whose stiffness is $k = 26480$ N/m and the initial tension is $F_0 = 123.6$ N, connects an upper thigh frame of the HAL to a lower thigh frame of it through a wire to play the alternative role of the muscle groups, such as the vastus lateralis, vastus intermedius, vastus medialis, etc.

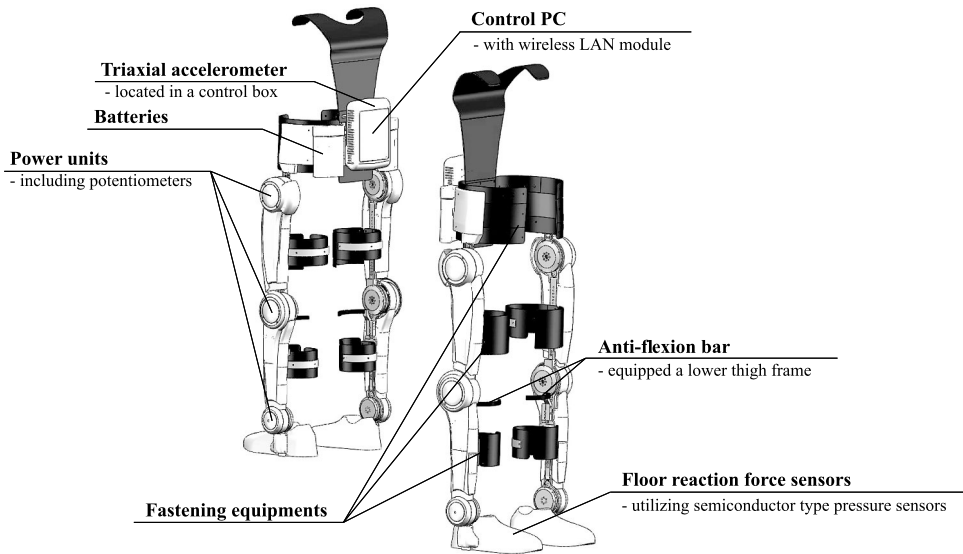


Figure 2. System configurations of HAL-5 LB ‘Type-C’.

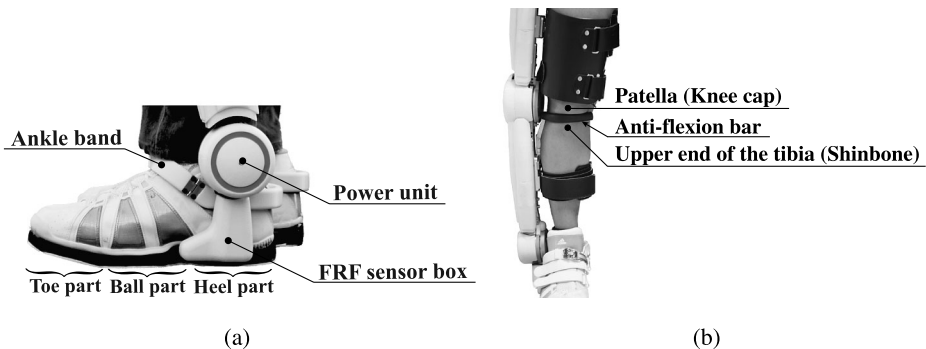


Figure 3. (a) Three FRF sensors that are embedded in the sole of the toe part, ball part and heel part. (b) Lower thigh part with anti-flexion bar for the knee joint. The anti-flexion bar covered with 5 mm thick rubber follows the frontal surface of the lower thigh in order to transmit the extension torque of the knee joint effectively to the wearer’s legs. In addition, the installation position of the bar is adjustable for wearers of various physiques.

3. Intention Estimation

3.1. Definition of Phases at the Desired Motion

We have proposed a ‘phase sequence’ concept that divides a sequence of a functional motion into motion elements in a short-term phase in order to comprehend and reconstruct a desired motion [5]. For example, a biped walk is divided into two phases from the viewpoint of contact conditions: single-support phase and double-support phase [15]. The gait can be divided into two phases from the viewpoint of

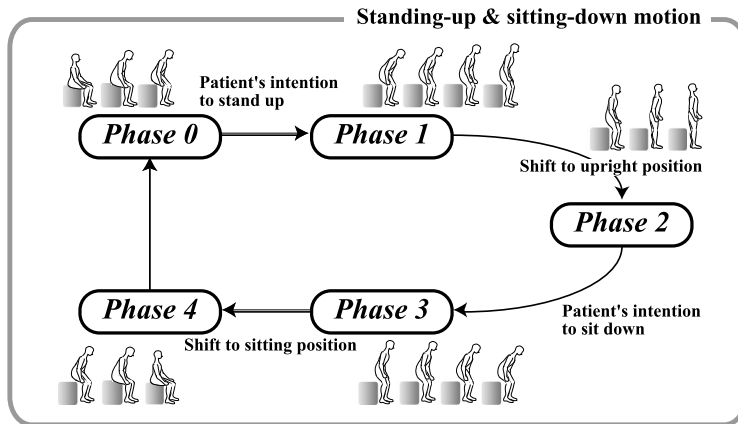


Figure 4. Definition of phases at the sit-to-stand and stand-to-sit transfers. In the ‘sitting phase’ a wearer is seated on a chair. The phase shifts to the following phase, the ‘sit-to-stand transfer phase’, when a wearer’s intention to stand up is observed. The next phase, the ‘standing phase’, starts when the wearer has an upright posture. Then, the phase shifts to the following phase, the ‘stand-to-sit transfer’, when the wearer’s intention to sit down is observed. Finally, the wearer sits on the chair in the ‘sitting phase’.

physical constraints: single-support phase and double-support phase. On the contrary, the sit-to-stand and stand-to-sit transfers including standing and sitting states immediately before and after the transfers are divided into five phases based on the posture conditions as shown in Fig. 4. In this case, conditions for phase change could explain each phase more explicitly than definitions of each phase. The conditions for phase change are defined as (Sections 3.2 and 3.3):

- (i) Inequalities (1), (2) and (3) are phase-change conditions from phase 0 to phase 1.
- (ii) Inequality (4) is a phase-change condition from phase 1 to phase 2.
- (iii) Inequality (5) is a phase-change condition from phase 2 to phase 3.
- (iv) Inequality (6) is a phase-change condition from phase 3 to phase 4.

A sit-to-stand transfer is divided into three phases: sitting phase (phase 0), sit-to-stand transfer phase (phase 1) and standing phase (phase 2). A stand-to-sit transfer is also divided into three phases: standing phase (phase 2), stand-to-sit transfer phase (phase 3) and sitting phase (phase 4). Phase-change conditions from phase 0 to phase 1 are the inclination angle of a patient’s upper body, COP position and FRF value because a human’s intention related to the sit-to-stand transfer is detected by the body inclination, COP transfer and increase of the FRF. A phase-change condition from phase 1 to phase 2 is the knee joint angle of a patient. A phase-change condition from phase 2 to phase 3 is the COP position because a human’s intention related to the stand-to-sit transfer is detected by the COP transfer. A phase-change condition from phase 3 to phase 4 is the knee joint angle of a patient.

3.2. Intention Estimation for the Sit-to-Stand Transfer

The ultimate interface that connects an exoskeletal assistive system with a wearer would be to directly convey the wearer's intention with regard to the desired motion to the assistive device. Detecting the form of electrical potential such as BES is one of the ways to infer the wearer's intention related to his/her motion. Unfortunately, the proper signals cannot be obtained from patients such as complete SCI patients. We propose another algorithm to infer the intention of the patient from the preliminary motion that is observed before the desired motion. As a result, the HAL starts the sit-to-stand and stand-to-sit transfers support synchronizing with the wearer's motion.

For sit-to-stand transfer, a person generally inclines their upper body forward in order to stably support their weight on the legs. The ground projection of the COG corresponds to the COP in static mode [16–18]. In addition, a FRF increases along with an anterior inclination of the body trunk [19, 20]. Using these phenomena, the patient's intention to stand up is detected by the body inclination, COP transfer and increase of the FRF. The patient, therefore, starts the sit-to-stand transfer without any operations, just by bending their upper body forward as the preliminary motion. The HAL estimates that a patient intends to stand up when the following inequalities are satisfied:

$$\theta_{\text{hip}} > \theta_{\text{thre1_hip}} \quad (1)$$

$$x_{\text{cop}} > x_{\text{thre1_cop}} \quad (2)$$

$$F > F_{\text{thre1_frf}}, \quad (3)$$

where θ_{hip} is the relative angle of hip joint as shown in Fig. 5, x_{cop} is the COP of the total system in the sagittal plane and F (N/kg) is a normalized value of the reaction forces measured by the FRF sensors. $\theta_{\text{thre1_hip}}$, $x_{\text{thre1_cop}}$ and $F_{\text{thre1_frf}}$ are thresholds to shift from phase 0 to phase 1. Phase 0 shifts to phase 1 once the intention to stand up is estimated. Next, phase 1 shifts to phase 2 when the following inequality is satisfied:

$$\theta_{\text{knee}} < \theta_{\text{thre2_knee}}, \quad (4)$$

where θ_{knee} is the relative angle of knee joint as shown in Fig. 5. $\theta_{\text{thre2_knee}}$ is the threshold to shift to phase 2. In phase 2, the HAL starts the standing phase.

3.3. Intention Estimation for the Stand-to-Sit Transfer

The patient's intention to sit down is detected by the COP transfer during the standing phase (phase 2). The patient, therefore, starts the stand-to-sit transfer just by transferring the COP either back or forth as the preliminary motion. The HAL estimates that a patient intends to sit down when the following inequality is satisfied:

$$x_{\text{ref_cop}} - x_{\text{cop}} > x_{\text{thre3_back}} \quad \text{OR} \quad x_{\text{cop}} - x_{\text{ref_cop}} > x_{\text{thre3_forth}}, \quad (5)$$

where $x_{\text{ref_cop}}$ is the reference of the COP during phase 2. $x_{\text{thre3_back}}$ and $x_{\text{thre3_forth}}$ are the thresholds of the COP in the back or forth direction, respectively. The patient

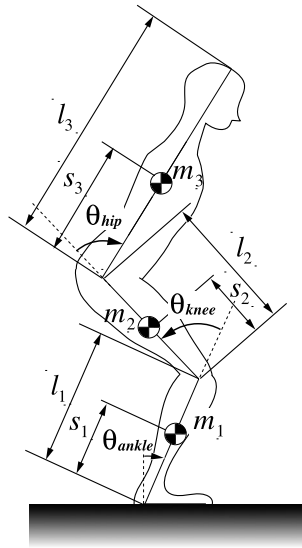


Figure 5. Definition of system parameters and variables. The flexion direction of each joint angle is set to be positive and each joint angle becomes 0 rad in an upright posture.

moves the COP either back and forth in order to shift to phase 3. Next, phase 3 shifts to phase 4 when the inequality below is satisfied:

$$\theta_{knee} > \theta_{thre4_knee}, \quad (6)$$

where θ_{thre4_knee} is the threshold of the knee joint angle to shift to phase 4. θ_{thre4_knee} is decided based on the knee joint angle that started the phase 1 so as to shift to the phase 4 immediately before the wearer's buttocks reach the surface of the chair. When the condition shown in inequality (6) is satisfied, the status shifts to the sitting posture phase (phase 4).

4. Controller Design

4.1. Control Strategy

The proposed support system includes two algorithms to support the patient's sit-to-stand and stand-to-sit transfers:

- Balance control algorithm based on the wearer's COP.
- Gravity compensation algorithm for weight bearing.

The torque of each joint of the HAL is calculated by considering two required algorithms: the balance control algorithm and the gravity compensation algorithm. The angles of the ankle joints have much influence on the position of the COP [21]. The range of the torque applied to the ankle joints is, however, limited because the feet start rotating around the tip of the toes or the heels. The hip joints in addition

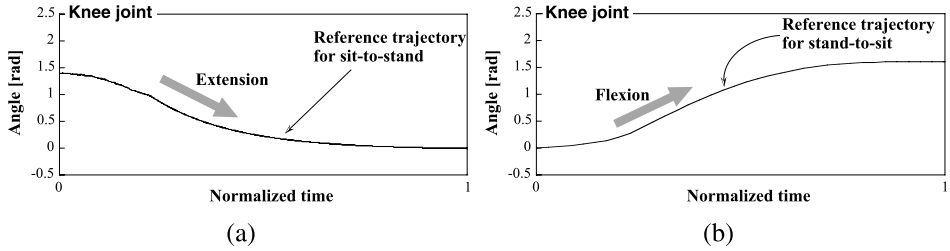


Figure 6. Reference patterns of knee joint angle: (a) during the sit-to-stand transfer and (b) during the stand-to-stand transfer.

to the ankle joints are used to control the position of the COP as the balance control. On the other hand, a height transition of the COG of a wearer as well as the position of the COP is very important for the wearer to feel comfortable during the motion support. The knee joints are used to control the height of the COG, because they directly contribute to the height of the COG. Additionally, it is necessary to provide necessary considerations for the wearers’ physical characteristic, so as not to give the wearer an uncomfortable feeling. Therefore, the reference trajectory of the height is extracted from a healthy person’s motion. The reference trajectories of the knee joint of the HAL shown in Fig. 6 are calculated based on the reference trajectories of the height during sit-to-stand and stand-to-sit transfers. The time period of the trajectories and the amplitude of the trajectories can be adjusted to the wearer’s physical characteristic, the degree of physical impairment and the wearer’s preference.

The ankle joint torques are the sum of the proportional and derivative (PD) control of the COP measured by the FRF sensors and the gravity compensation as shown in (7). The COP control and the gravity compensation are explained in the following subsections. The hip joint torques are the sum of the PD control of the COP and the gravity compensation as shown in (8). The reference angle of the hip joint θ_{ref_hip} is calculated from the kinetic model as shown in Fig. 5 such that the current COP goes toward the reference position of the COP. The detail is explained in the next subsection. The knee joint torques are the sum of the PD control using the reference pattern based on a healthy person’s knee trajectory and the gravity compensation as shown in (9):

$$\tau_{ankle} = \mathbf{KPa}(x_{ref_cop} - x_{cop}) - \mathbf{KD}_a \dot{x}_{cop} + \tau'_{ankle} \tag{7}$$

$$\tau_{hip} = \mathbf{KPh}(\theta_{ref_hip} - \theta_{hip}) - \mathbf{KDh} \dot{\theta}_{hip} + \tau'_{hip} \tag{8}$$

$$\tau_{knee} = \mathbf{KPk}(\theta_{ref_knee} - \theta_{knee}) - \mathbf{KDk} \dot{\theta}_{knee} + \tau'_{knee}, \tag{9}$$

where τ_{ankle} , τ_{hip} , τ_{knee} , τ'_{ankle} , τ'_{hip} , τ'_{knee} , x_{cop} , θ_{hip} , θ_{knee} , \dot{x}_{cop} , $\dot{\theta}_{hip}$, $\dot{\theta}_{knee}$, x_{ref_cop} , θ_{ref_hip} and θ_{ref_knee} are column matrices. These variables have two elements that corresponded to right and left legs. Feedback gains \mathbf{KPa} , \mathbf{KD}_a , \mathbf{KPh} , \mathbf{KDh} , \mathbf{KPk} and \mathbf{KDk} are diagonal matrices where feedback gains for each leg are diagonal elements.

They are expressed as:

$$\begin{aligned} \mathbf{K}_{Pa} &= \begin{bmatrix} K_{PaR} & 0 \\ 0 & K_{PaL} \end{bmatrix}, & \mathbf{K}_{Da} &= \begin{bmatrix} K_{DaR} & 0 \\ 0 & K_{DaL} \end{bmatrix} \\ \mathbf{K}_{Ph} &= \begin{bmatrix} K_{PhR} & 0 \\ 0 & K_{PhL} \end{bmatrix}, & \mathbf{K}_{Dh} &= \begin{bmatrix} K_{DhR} & 0 \\ 0 & K_{DhL} \end{bmatrix} \\ \mathbf{K}_{Pk} &= \begin{bmatrix} K_{PkR} & 0 \\ 0 & K_{PkL} \end{bmatrix}, & \mathbf{K}_{Dk} &= \begin{bmatrix} K_{DkR} & 0 \\ 0 & K_{DkL} \end{bmatrix}, \end{aligned} \quad (10)$$

where subscripts Pa_R , Pa_L , Ph_R , Ph_L , Pk_R and Pk_L are the proportional gain of the right ankle joint, the left ankle joint, the right hip joint, the left hip joint, the right knee joint and the left knee joint, respectively. Da_R , Da_L , Dh_R , Dh_L , Dk_R and Dk_L are the derivative gain of the right ankle joint, the left ankle joint, the right hip joint, the left hip joint, the right knee joint and the left knee joint, respectively.

4.2. Balance Control Algorithm Based on the Wearer's COP

Balance control is absolutely essential for safer physical support. In the field of a humanoid robots, many control strategies for balance maintenance have been proposed [22–26]. The balance of a humanoid robot within the support polygon is usually maintained by controlling the position of the zero moment point (ZMP). The ZMP is mainly used as a standard evaluation index of the stability of the robot. The ZMP also corresponds to the COP [16–18]. In this paper, therefore, the HAL controls the wearer's COP during the sit-to-stand and stand-to-sit transfers.

Three FRF sensors are installed in the toe part, ball part and heel part of the sole one by one. The transfers in this paper are quasi-static motions. The COP of the right foot C_r and the left foot C_l are calculated by:

$$C_r = \frac{f_{rt}x_{rt} + f_{rb}x_{rb} + f_{rh}x_{rh}}{f_{rt} + f_{rb} + f_{rh}} \quad \text{and} \quad C_l = \frac{f_{lt}x_{lt} + f_{lb}x_{lb} + f_{lh}x_{lh}}{f_{lt} + f_{lb} + f_{lh}}, \quad (11)$$

where f_{rt} , f_{rb} , f_{rh} , f_{lt} , f_{lb} and f_{lh} are the reaction forces measured by the FRF sensors of the toe part, the ball part and the heel part of the right sole and the left sole, respectively. x_{rt} , x_{rb} , x_{rh} , x_{lt} , x_{lb} and x_{lh} are sensor positions in the sagittal plane of the toe part, the ball part and the heel part of the right sole and the left sole, respectively. The COP of the total system in the sagittal plane x_{cop} is calculated by:

$$x_{cop} = \frac{(f_{rt} + f_{rb} + f_{rh})C_r + (f_{lt} + f_{lb} + f_{lh})C_l}{f_{rt} + f_{rb} + f_{rh} + f_{lt} + f_{lb} + f_{lh}}. \quad (12)$$

According to biomechanical analysis, the COP of a healthy person is located around the ankle joint axis from the viewpoint of the ankle joint torque [27]. In this study, however, the reference position of the COP x_{ref_cop} is located 10–20 cm in front of the ankle joint axis from the viewpoint of the stability margin. The ankle joints are directly controlled based on the error of the COP position as shown in the first term on the right side of (7).

The hip joints are also controlled based on the COP. The reference angle of the hip joints, however, is calculated from the kinetic model as shown in Fig. 5, in order to absorb the offset caused by the difference between individual physical parameters. In addition, the hip joints are controlled based on the angular error of the hip joint as shown in the first term on the right side of (8). The position of COP in the sagittal plane x'_{cop} is calculated based on a direct kinematics method expressed by:

$$x'_{\text{cop}} = \frac{1}{m_1 + m_2 + m_3} \left\{ (m_1 s_1 + m_2 l_1 + m_3 l_1) \cos\left(\frac{\pi}{2} - \theta_{\text{ankle}}\right) - (m_2 s_2 + m_3 l_2) \cos\left(\frac{\pi}{2} - \theta_{\text{ankle}} + \theta_{\text{knee}}\right) + m_3 s_3 \cos\left(\frac{\pi}{2} - \theta_{\text{ankle}} + \theta_{\text{knee}} - \theta_{\text{hip}}\right) \right\}, \quad (13)$$

where θ_{ankle} is the relative angle of ankle joint as shown in Fig. 5, m_i is the mass of link i , s_i is the position of mass i and l_i is the link length, respectively. The inverse kinematics of the hip joint angle θ_{hip} are solved by using (13). The reference angle of the hip joint $\theta_{\text{ref_hip}}$ is obtained uniquely, if the reference position of the COP $x'_{\text{ref_cop}}$ is substituted for x'_{cop} . Therefore, $\theta_{\text{ref_hip}}$ is obtained by:

$$\theta_{\text{ref_hip}} = \frac{\pi}{2} - \theta_{\text{ankle}} + \theta_{\text{knee}} - \cos^{-1} \left[\frac{1}{m_3 s_3} \left\{ (m_1 + m_2 + m_3) x'_{\text{ref_cop}} + (m_2 s_2 + m_3 l_2) \cos\left(\frac{\pi}{2} + \theta_{\text{ankle}} - \theta_{\text{knee}}\right) - (m_1 s_1 + m_2 l_1 + m_3 l_1) \cos\left(\frac{\pi}{2} - \theta_{\text{ankle}}\right) \right\} \right]. \quad (14)$$

The reference hip joint angle $\theta_{\text{ref_hip}}$ shown in (14) is updated at each control cycle based on the current other joint angles.

4.3. Gravity Compensation Algorithm for Weight Bearing

The high gains of the PD control in (7)–(9) are necessary in order to lower the errors from the reference angles if a constant large force such as gravity affects the system joints. The gravity compensation of the patient’s weight and the system’s mass enables us to fix lower gains of the PD control so that the stiffness of the system joints could be lower. That contributes to supporting the patient’s motions with flexibility. The gravity compensation torque of each joint is calculated by:

$$\tau'_{\text{ankle}} = - \left\{ (m_1 s_1 + m_2 l_1) g \cos\left(\frac{\pi}{2} - \theta_{\text{ankle}}\right) + (m_2 s_2 + m_3 l_2) g \cos\left(\frac{\pi}{2} - \theta_{\text{ankle}} + \theta_{\text{knee}}\right) + m_3 s_3 g \cos\left(\frac{\pi}{2} - \theta_{\text{ankle}} + \theta_{\text{knee}} - \theta_{\text{hip}}\right) \right\} \quad (15)$$

$$\tau'_{\text{hip}} = -m_3 s_3 g \cos\left(\frac{\pi}{2} - \theta_{\text{ankle}} + \theta_{\text{knee}} - \theta_{\text{hip}}\right) \quad (16)$$

$$\tau'_{\text{knee}} = -\left\{ (m_3 l_2 + m_2 s_2) g \cos\left(\frac{\pi}{2} - \theta_{\text{ankle}} + \theta_{\text{knee}}\right) + m_3 s_3 g \cos\left(\frac{\pi}{2} - \theta_{\text{ankle}} + \theta_{\text{knee}} - \theta_{\text{hip}}\right) \right\}, \quad (17)$$

where g is the gravitational acceleration.

5. Experiments

The proposed algorithms for the sit-to-stand and stand-to-sit transfer support are verified through experiments that are separately executed in two steps from the viewpoint of safety. In the first step, parameters of the control algorithms are adjusted through a preliminary experiment because stiffness and damping factors of a human body could not be modeled precisely. A healthy person wearing the HAL simulates the conditions of a patient who has completely impaired motor and sensory functions of the lower limbs. He, however, keeps his body balance by himself, controlling his lower limbs in unexpected situations. The experiment for parameter settings could be conducted safely, thanks to the high adaptability of the healthy person. In the following step, the patient safely receives the motion support from the HAL without overshooting from the beginning of the clinical trial by using the adjusted parameters.

5.1. Preliminary Experiment

5.1.1. Experiment Settings

A healthy person who has similar physical parameters to the patient was adopted as a subject in the preliminary experiment. The HAL's weight of each link is measured in advance. However, the precise wearer's weight of each body segment is not measurable. In order to apply the gravity compensation algorithm to the patient with the HAL, the wearer's weights of each body segment are necessary as well as the HAL's weights of each link. The mean values of elderly Japanese men from statistics as shown in Table 1 are, therefore, used for the balance control algorithm and the gravity compensation algorithm. The values are previously calibrated by the

Table 1.
Parameter settings of the patient

Mass (kg)		Length (m)		Length (m)	
m_1	6.62	s_1	0.25	l_1	0.45
m_2	6.64	s_2	0.2	l_2	0.35
m_3	48.00	s_3	0.45	l_3	0.80

experiment so as not to give an uncomfortable feeling to the wearer. The healthy person completely relaxes his legs to simulate the lower limb functions of the patient who has completely impaired motor and sensory functions of the lower limbs. The proportional gains K_{Ph_*} , K_{Pk_*} and K_{Pa_R} and derivative gains K_{Dh_*} , K_{Dk_*} and K_{Da_R} used in the feedback control (10) are adjusted so that each joint could follow the reference trajectory without overshooting.

5.1.2. Results

The PD gains of each phase were adjusted in the preliminary experiment. Figure 7 shows the angles of the hip and knee joints, the COP trajectory, and those references through three phases during sit-to-stand transfer support. These graphs show that the angles of the hip and knee joints and the COP follow the references without overshooting when the feedback gains are set as $K_{Ph_*} = 100.0$, $K_{Dh_*} = 3.5$, $K_{Pk_*} = 130.0$, $K_{Dk_*} = 3.5$, $K_{Pa_*} = 18.0$ and $K_{Da_*} = 8.0$. Those gains are fixed in phase 1, phase 2 and phase 3.

5.2. Clinical Trial

5.2.1. Experimental Environment

In this paper, proposed algorithms are applied to a paraplegic patient. The participant is a 66-years-old male, 160 cm tall and his weight is 68 kg. He is diagnosed with complete SCI because the T10 and T11 thoracic vertebrae are damaged due to vertebral fracture. He can control his posture using parallel bars with both his arms so as to convey his intention related to the sit-to-stand and stand-to-sit transfers as shown in Fig. 8. Additionally, a horizontal bar is fixed to the parallel bars at a height of 90 cm in front of the patient so that he can grip the bar in an unexpected situation such as an emergency fall. The waist sling installed on his torso is connected to a hoist. However, the belt that connects the hoist with the waist sling is normally slack so as not to disturb sit-to-stand and stand-to-sit transfers of the patient. In addition, the height of the chair has the greatest influence on the motion support because the knee flexion moment is reduced by raising the height of a chair [28]. In this clinical trial, the height of the chair was set at the height that corresponds to 100% (45 cm height) of the length of the patient's lower thigh. The chair is fixed to the hoist to make sure it does not move during the motion support.

The patient gave informed consent before participating in this clinical trial. All procedures were approved by the 'Institutional Review Board' and this clinical trial was conducted under the inspection of a medical doctor. The physical condition of his lower limbs was examined by a medical doctor just before every trial. Furthermore, the maximum velocity of reference knee joints angles was adjusted in advance to prevent muscle spasm from developing during the clinical trial. After the preparations mentioned above, muscle spasticity in his lower limbs, which might restrict the use of the system, was not observed during the clinical trial.

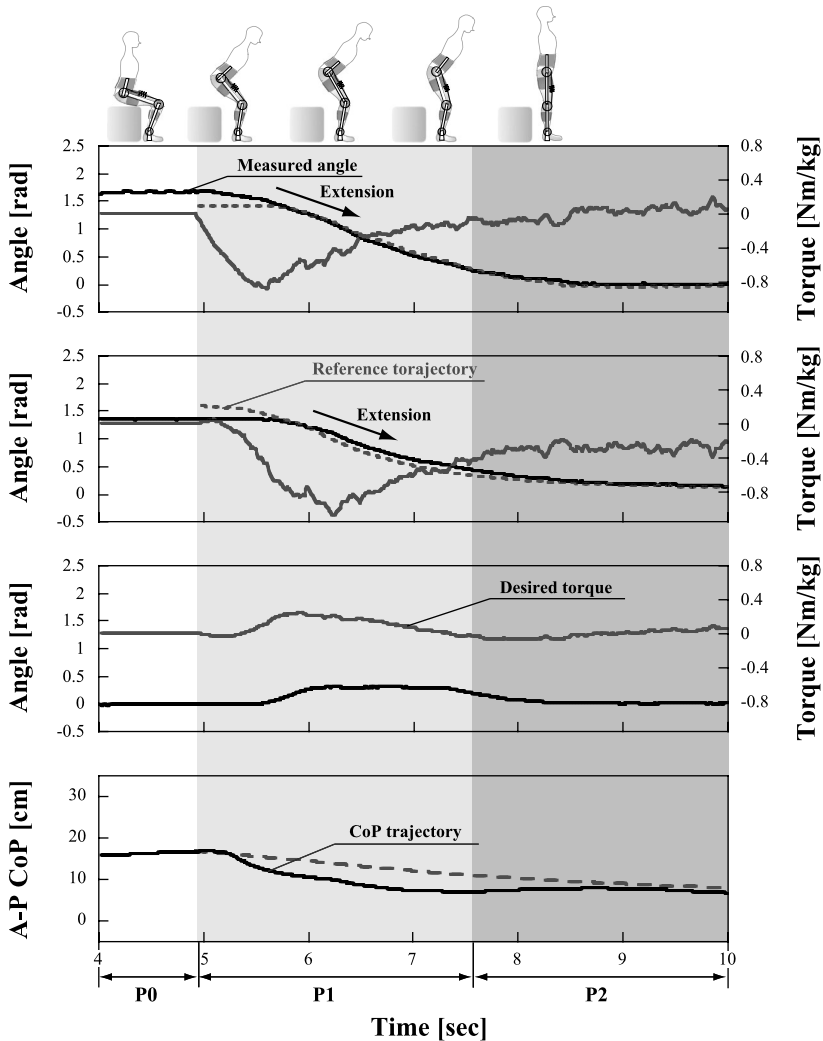


Figure 7. Result of the preliminary experiment. These graphs show the angle and torque of each joint and the COP calculated by the FRF sensors in the A–P direction through three phases. The desired torque of each joint is calculated using (7), (8) and (9). The torque of each joint is a normalized value based on the weight of the total system. P0 (white area), P1 (light gray area) and P2 (gray area) denote the phase of sitting, sit-to-stand transfer and standing, respectively. Dashed lines represent the reference trajectories. The ankle joint is controlled so that the current COP of the total system could follow the reference of the COP. On the other hand, the reference trajectory of the knee joints is calculated based on a healthy person’s sit-to-stand transfer. The reference angle of the hip joint is calculated based on the angles of the ankle joint and the knee joint using (14).

5.2.2. Results

We verified the performance of the proposed algorithms including the intention estimation algorithm through a clinical trial with the complete SCI patient. Figure 9

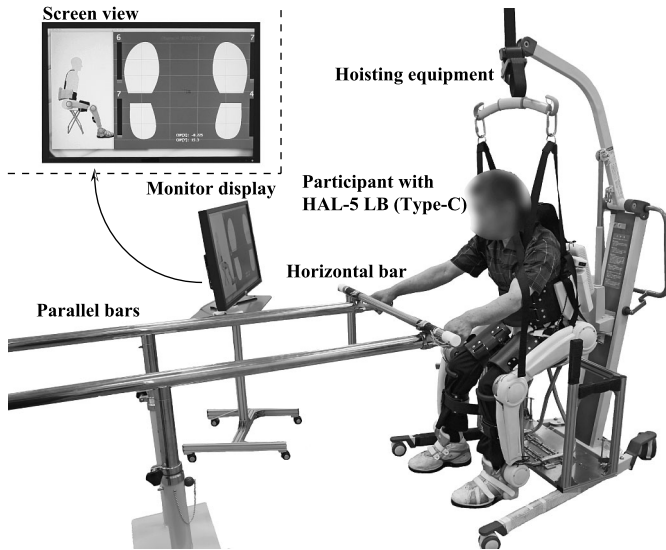


Figure 8. Experimental environment of the clinical trial. A hoist is connected to the waist of the patient through a slack sling so that the hoist could prevent the patient from falling down in the case of system failure. Joint angles of the wearer's lower limbs and the COP of the total system are displayed on a monitor display during sit-to-stand and stand-to-sit transfers.

shows the angles and torques of each joint, the FRFs and the COP through three phases during sit-to-stand transfer. The results in these graphs indicate that the hip and knee joints follow the reference trajectories. In addition, the COP also follows the reference trajectory. The COP in the anterior–posterior (A–P) and medial–lateral (M–L) directions during sit-to-stand transfer is shown in Fig. 10. After the buttocks left the seating surface (phase 1), the system is able to control the COP of the total system within 38.2–58.7% of the support polygon in the A–P direction from 3.8 to 6.8 s. After the sit-to-stand transfer was completed (phase 2), the system is able to control the COP within 31.8–38.2% of the support polygon in the A–P direction from 6.8 to 16.0 s. These results indicate that the COP control keeps the stability of his balance during sit-to-stand transfer support.

Figure 11 shows the COP trajectory and the phase transitions at the start of the stand-to-sit transfer. In order to start the stand-to-sit transfer phase during phase 2, the wearer shifts his COP backward by pushing his upper body with his arms slightly. The HAL estimates that he intends to sit down from a standing posture when inequality (5) is satisfied. Then, the HAL starts his stand-to-sit transfer support, synchronizing his intention. Figure 12 shows the angles and torques of each joint and the COP through three phases during stand-to-sit transfer support. The results in these graphs indicate that the hip and knee joints follow the reference trajectories. The COP also follows the reference trajectory. The COP in the A–P and M–L directions during stand-to-sit transfer is shown in Fig. 13. In phase 2, the system is able to control the COP within 21.3–35.6% of the support polygon in the

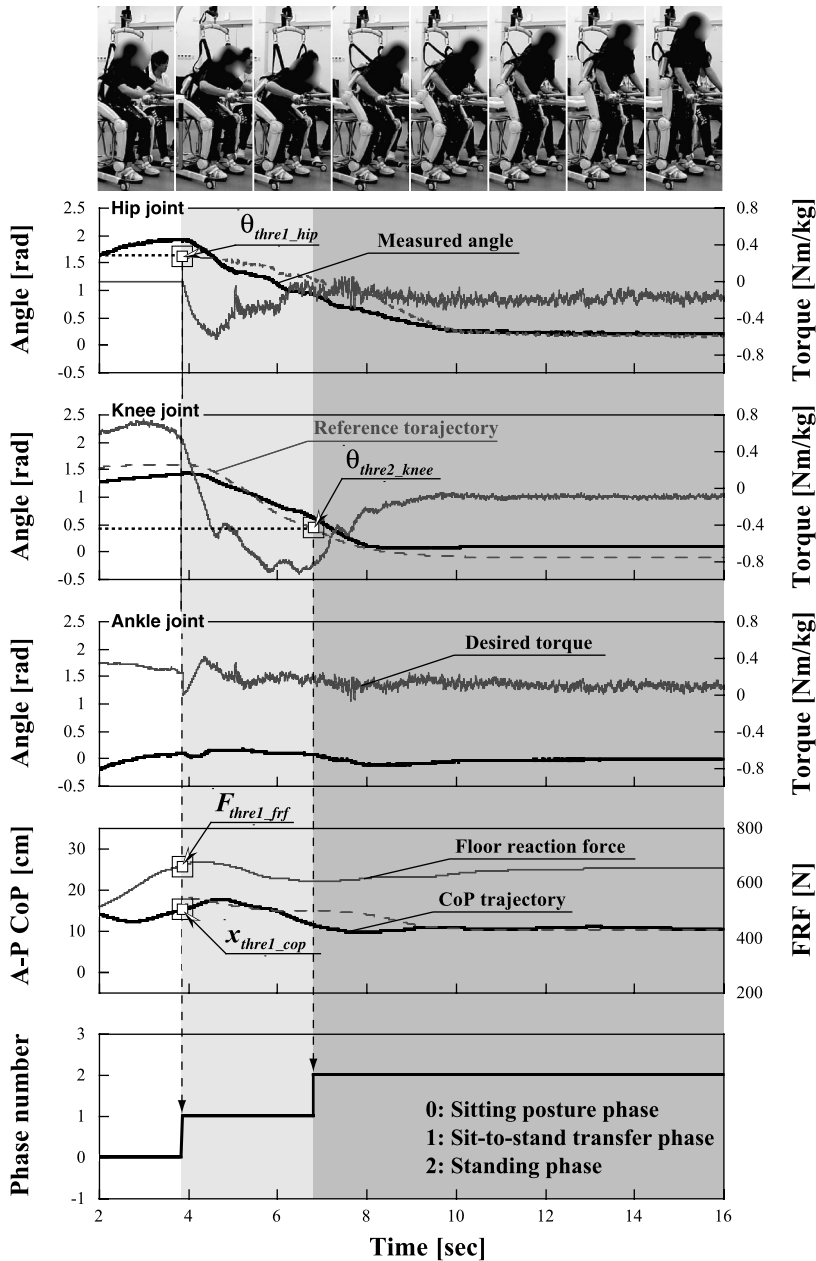


Figure 9. Result of the sit-to-stand transfer support in the clinical trial. These graphs show the angle and torque of each joint, the FRFs, and the COP calculated by the FRF sensors in the A–P direction through three phases. The desired torque of each joint is calculated using (7)–(9). The HAL estimated that the wearer intends to stand up from a sitting posture when inequalities (1)–(3) were satisfied at 3.8 s. At that time, the HAL started the sit-to-stand transfer phase (phase 1). Next, when inequality (4) was satisfied during phase 1, the standing phase (phase 2) started at 6.8 s.

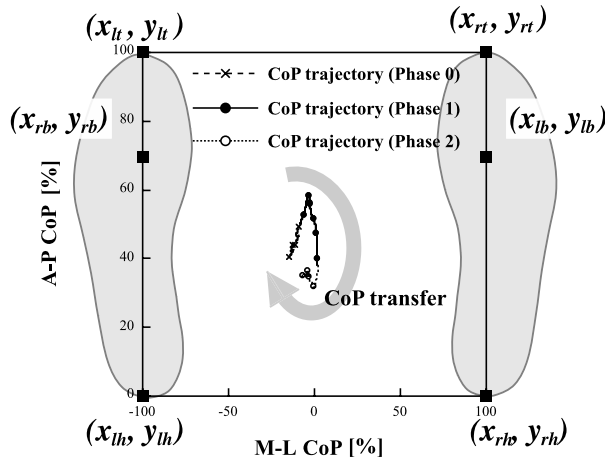


Figure 10. COP trajectory of the support polygon in the A–P and M–L directions during sit-to-stand transfer support.

A–P direction from 18.0 to 19.7 s. In phase 3, the system is able to control the COP within 17.7–37.9% of the support polygon in the A–P direction from 19.7 to 26.5 s. These results indicate that the COP control keeps the stability of his balance during stand-to-sit transfer support.

Figure 14a shows the mean position of the COP in the A–P direction from phase 1 to phase 2 when the wearer received the sit-to-stand transfer support from the HAL while looking at the monitor that shows the current COP and joint angles of the wearer’s lower limbs. The proposed support system can control the COP at 39.7% (standard deviation: 9.71%) on average. As shown in Fig. 14b, the system controls the COP at 40.1% (standard deviation: 13.04%) on average when he received the sit-to-stand transfer support from the HAL without looking at the monitor. Figure 15a shows the mean position of the COP in the A–P direction from phase 2 to phase 3, when the wearer received the stand-to-sit transfer support from the HAL while looking at the monitor. The system can control the COP at 32.4% (standard deviation: 7.95%) on average. As shown in Fig. 15b, the system controls the COP at 25.3% (standard deviation: 10.31%) when he received the stand-to-sit transfer support from the HAL without looking at the monitor. The results mean that the patient who confirms his current COP depicted on the monitor could control his balance by himself during the transfers cooperating with the HAL so that stability and safety could be increased.

6. Discussion

Physical support during sit-to-stand and stand-to-sit transfers is important for the independent life of paraplegic patients. In particular, we focused on the motion support for complete paraplegic patients. Although an assistive system should start

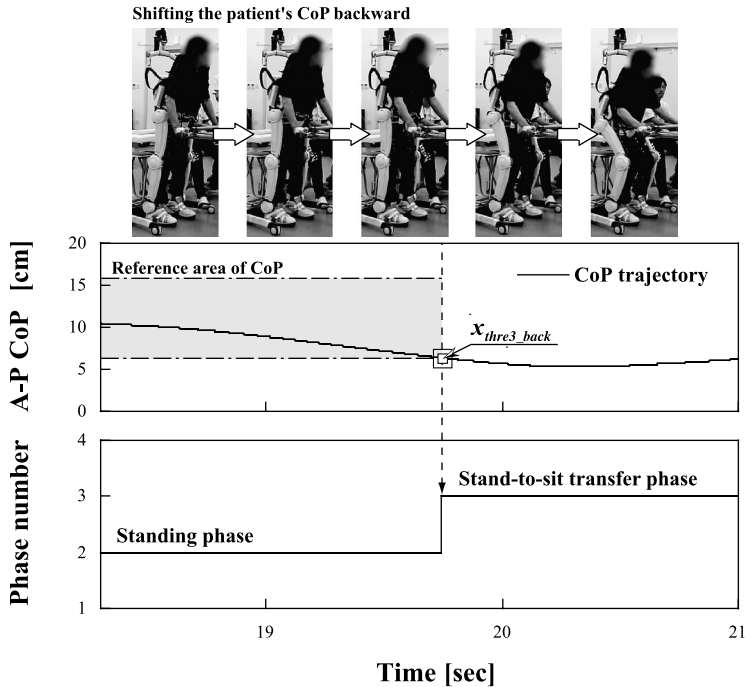


Figure 11. Detection of the wearer's intention to sit down. Sequential photographs show how the wearer pushes the parallel bars with his arms to convey his intention related to sit down to the HAL and that he starts the stand-to-sit transfer. In phase 2, the COP of the total system was controlled within the range of the reference COP indicated in the gray area. After that, he shifted the COP to the threshold x_{thre3_back} at 19.7 s in order to start the stand-to-sit transfer. Then, the HAL started supporting his stand-to-sit transfer, synchronizing his intention. The range of the reference COP in the A–P direction is set from 6.35 to 15.4 cm based on the result of the preliminary experiment empirically.

supporting the motions at the proper moment synchronizing the patient's intention to stand up and to sit down, it has not yet been solved. The purpose of this study was to realize the control method of complete paraplegic patients during sit-to-stand and stand-to-sit transfers through an intuitive interface.

To achieve this purpose, we proposed the algorithms to support the wearer's weight and body posture for stability, and to infer the intention based on a preliminary motion that is observed just before sit-to-stand and stand-to-sit transfers. The proposed algorithms embedded in the HAL were applied to a complete SCI patient who is able to shift his COG by using upper body functions including arms and hands. The physical condition of the wearer's lower limbs should be examined before its use so as to prevent any muscle spasm from developing.

In the clinical trial, we confirmed that the wearer could intuitively start the sit-to-stand and stand-to-sit transfer support based on a preliminary motion of his upper body instead of his bioelectrical signals. The HAL detected the wearer's intention to stand up from the preliminary motions of his body trunk inclining forward and

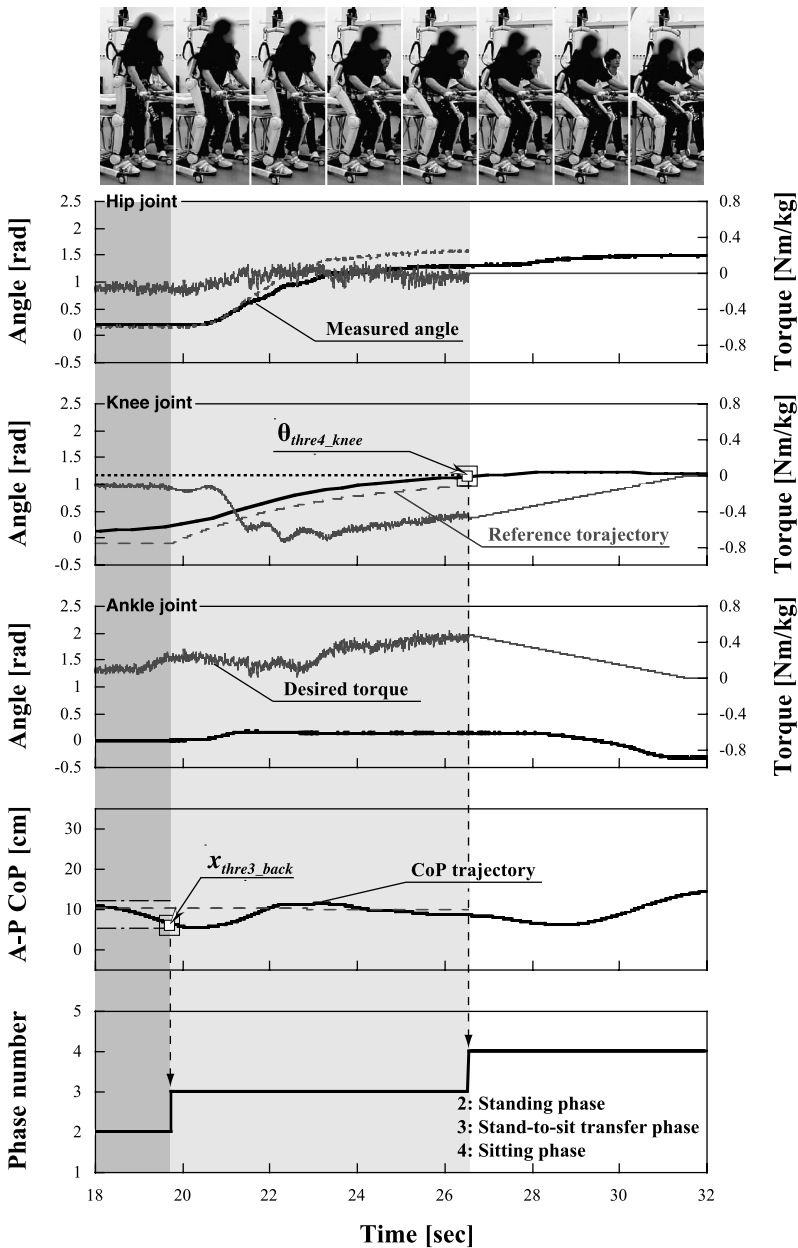


Figure 12. Result of the stand-to-sit transfer support in the clinical trial. These graphs show the angle and torque of each joint and the COP calculated by the FRF sensors in the A–P direction through three phases. The HAL estimated that the wearer intends to sit down when the conditions shown in inequality (5) was satisfied (19.7 s). At that time, the HAL started the stand-to-sit transfer phase (phase 3). Next, when the condition shown in inequality (6) was satisfied during phase 3, the phase shifted to the sitting phase (phase 4) at 26.5 s. In phase 4, the torque of each joint of the HAL is designed to decrease gradually so that the wearer could smoothly sit on the chair.

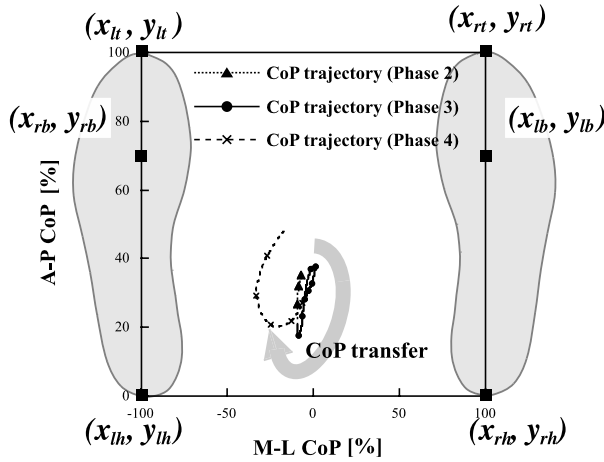


Figure 13. COP trajectory of the support polygon in the A–P and M–L directions during stand-to-sit transfer support.

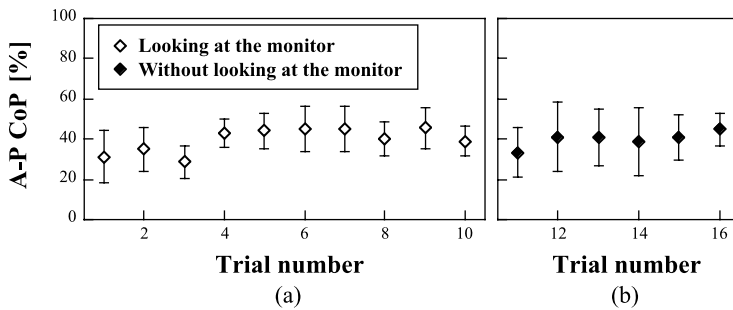


Figure 14. Mean position of the COP of the support polygon in the A–P direction during sit-to-stand transfer support: (a) while looking at the monitor and (b) without looking at the monitor.

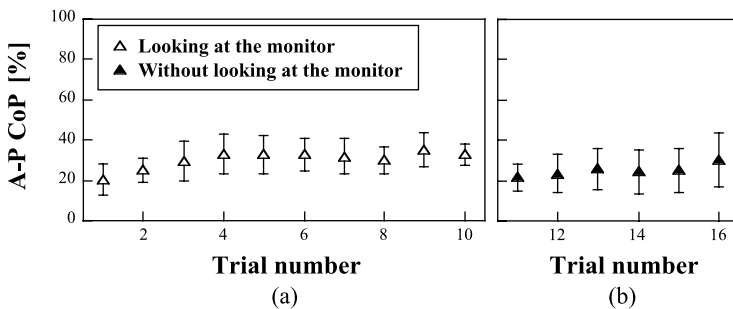


Figure 15. Mean position of the COP of the support polygon in the A–P direction during stand-to-sit transfer support: (a) while looking at the monitor and (b) without looking at the monitor.

the COP exceeding the threshold, and it autonomously supported the patient's sit-to-stand transfer. In addition, the HAL detected the wearer's intention to sit down from the preliminary motions that made the COP go backward out of the support polygon when the wearer pushed his upper body with his arms during the standing phase (phase 2). After that, the HAL autonomously supported the patient's stand-to-sit transfer. These results indicated that the proposed algorithms successfully estimated his intention to stand up and to sit down.

During sit-to-stand transfer, the proposed system controlled the COP from 17.6 to 55.6% of the support polygon in the A–P direction as shown in Fig. 14a. During stand-to-sit transfer, the proposed system controlled the COP from 12.7 to 43.7% of the support polygon in the A–P direction as shown in Fig. 15a. The current COP information depicted on the monitor in front of the patient contributes to the precision of COP control in both transfers from the viewpoint of the standard deviations of the COP as shown in Figs 14b and 15b.

The most significant factor of these improvements is that the patient could understand the current condition of his balance from the monitor instead of the sensory feedback from the lower limbs. We are developing an auditory feedback system for complete paraplegic patients that would have practical implications in daily life, because the visual feedback occupies a patient's vision for interaction with his environment.

7. Conclusions

We proposed an algorithms to support the wearer's weight and to control the wearer's body posture for stability during sit-to-stand and stand-to-sit transfers. In addition, we proposed an algorithm to estimate the wearer's intention to start these motions based on a preliminary motion of their upper body and posture condition. In a clinical trial with a complete SCI patient, we confirmed that the proposed algorithms support sit-to-stand and stand-to-sit transfers of the patient with the HAL safely and conveniently by keeping his stability and by reflecting his intentions. The results of this study show that we realized the control method of complete paraplegic patients during sit-to-stand and stand-to-sit transfers by using the proposed algorithms.

Acknowledgements

This study was supported in part by the Grant-in-Aid for the Global COE Program on 'Cybernetics: fusion of human, machine, and information systems' at the University of Tsukuba, and by the Grant-in-Aid for Research on medical devices for analyzing, supporting and substituting the function of the human body, Ministry of Health, Labour and Welfare of Japan.

References

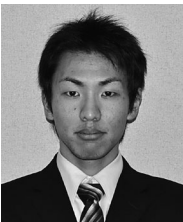
1. S. Goemaere, M. Van Laere, P. De Neve and J. M. Kaufman, Bone mineral status in paraplegic patients who do or do not perform standing, *Osteoporosis Int.* **4**, 138–143 (1994).
2. S. Lee and Y. Sankai, Power assist control for walking aid with HAL-3 based on EMG and impedance adjustment around knee joint, in: *Proc. IEEE/RSJ Int. Conf. on Intelligent Robots and Systems*, Lausanne, pp. 1499–1504 (2002).
3. K. Suzuki, Y. Kawamura, T. Hayashi, T. Sakurai, Y. Hasegawa and Y. Sankai, Intention-based walking support for paraplegia patient, in: *Proc. IEEE Int. Conf. on Systems, Man and Cybernetics*, Waikoloa, HI, pp. 2707–2713 (2005).
4. K. Suzuki, G. Mito, H. Kawamoto, Y. Hasegawa and Y. Sankai, Intention-based walking support for paraplegia patients with robot suit HAL, *Adv. Robotics* **21**, 1441–1469 (2007).
5. H. Kawamoto and Y. Sankai, Power assist method based on phase sequence and muscle force condition for HAL, *Adv. Robotics* **19**, 717–734 (2005).
6. F. Previdi, M. Ferrarin, S. M. Savaresi and S. Bittanti, Closed-loop control of FES supported standing up and sitting down using Virtual Reference Feedback Tuning, *Control Eng. Pract.* **13**, 1173–1182 (2005).
7. R. Riener, M. Ferrarin, E. E. Pavan and C. A. Frigo, Patient-driven control of FES-supported standing up and sitting down: experimental results, *IEEE Trans. Rehabil. Eng.* **8**, 523–529 (2000).
8. R. Kamnik and T. Bajd, Robot assistive device for augmenting standing-up capabilities in impaired people, in: *Proc. IEEE/RSJ Int. Conf. on Intelligent Robot and Systems*, Las Vegas, NV, pp. 3606–3611 (2003).
9. R. Kamnik and T. Bajd, Human voluntary activity integration in the control of a standing-up rehabilitation robot: a simulation study, *Med. Eng. Phys.* **29**, 1019–1029 (2007).
10. K. Nagai, I. Nakanishi and H. Hanabusa, Assistance of self-transfer of patients using a power-assisting device, in: *Proc. IEEE Int. Conf. on Robotics and Automation*, Taipei, vol. 3, pp. 4008–4015 (2003).
11. D. Chugo, W. Matsuoka, S. Jia and K. Takase, Rehabilitation walker with standing-assistance device, *Robotics Mechatron.* **19**, 604–611 (2007).
12. M. Tomita, T. Ogiso, Y. Nemoto and M. G. Fujie, A study on the path of an upper-body support arm used for assisting standing-up and sitting-down motion, *JSME Int. J.* **43**, 949–956 (2000).
13. A. Fattah, S. K. Agrawal, G. Catlin and J. Hamnett, Design of a passive gravity-balanced assistive device for sit-to-stand tasks, *Mech. Des. Trans. ASME* **128**, 1122–1129 (2006).
14. T. Noritsugu, D. Sasaki, M. Kameda, A. Fukunaga and M. Takaiwa, Wearable power assist device for standing up motion using pneumatic rubber artificial muscles, *Robotics Mechatron.* **19**, 619–628 (2007).
15. Q. Huang, K. Kaneko, K. Yokoi, S. Kajita, T. Kotoku, N. Koyachi, H. Arai, N. Imamura, K. Komoriya and K. Tanie, Balance control of a biped robot combining off-line pattern with real-time modification, in: *Proc. IEEE Int. Conf. on Robotics and Automation*, San Francisco, CA, pp. 3346–3352 (2000).
16. A. Goswami, Postural stability of biped robots and the foot-rotation indicator (FRI) point, *Int. J. Robotics Res.* **18**, 523–533 (1999).
17. L. Mouchnino, M. L. Mille, M. Cincera, A. Bardot, A. Delarque, A. Pedotti and J. Massion, Postural reorganization of weight-shifting in below-knee amputees during leg raising, *Exp. Brain Res.* **121**, 205–214 (1998).
18. S. Ito and H. Kawasaki, A standing posture control based on ground reaction force, in: *Proc. IEEE/RSJ Int. Conf. on Intelligent Robots and Systems*, Takamatsu, pp. 1340–1345 (2000).

19. F. Bahrami, R. Riener, P. Jabedat-Maralani and G. Schmidt, Biomechanical analysis of sit-to-stand transfer in healthy and paraplegic subjects, *Clin. Biomech.* **15**, 123–133 (2000).
20. E. Papa and A. Cappozzo, A telescopic inverted-pendulum model of the musculo-skeletal system and its use for the analysis of the sit-to-stand motor task, *Biomechanics* **32**, 1205–1212 (1999).
21. F. B. Horak and L. M. Nashner, Central programming of postural movements: adaptation to altered support-surface configurations, *Neurophysiol.* **55**, 1369–1381 (1986).
22. S. Kajita, F. Kanehiro, K. Kaneko, K. Fujiwara, K. Harada, K. Yokoi and H. Hirukawa, Biped walking pattern generation by using preview control of zero-moment point, in: *Proc. IEEE Int. Conf. on Robotics and Automation*, Taipei, pp. 1620–1626 (2003).
23. N. Nazir, S. Nakaura and M. Sampei, Balance control analysis of humanoid robot based on ZMP feedback control, in: *Proc. IEEE/RSJ Int. Conf. on Intelligent Robots and Systems*, Lausanne, pp. 2437–2442 (2002).
24. J. H. Park and H. Chung, ZMP compensation by on-line trajectory generation for biped robots, in: *Proc. IEEE Int. Conf. on Systems, Man and Cybernetics*, Tokyo, pp. 960–965 (1999).
25. S. Aoi and K. Tsuchiya, Locomotion control of a biped robot using nonlinear oscillators, *Autonomous Robots* **19**, 219–232 (2005).
26. A. Goswami, Foot rotation indicator (FRI) point: a new gait planning tool to evaluate postural stability of biped robots, in: *Proc. IEEE Int. Conf. on Robotics and Automation*, Detroit, MI, pp. 47–52 (1999).
27. V. S. Gurfinkel, Yu. P. Ivanenko, Yu. S. Levik and I. A. Babakova, Kinesthetic reference for human orthograde posture, *Neuroscience* **68**, 229–243 (1995).
28. M. W. Rodosky, T. P. Andriacchi and G. B. J. Andersson, The influence of chair height on lower limb mechanics during rising, *Orthopaed. Res.* **7**, 266–271 (1989).

About the Authors



Atsushi Tsukahara received the BE degree from College of Industrial Technology, Nihon University, Japan, in 2005, and the ME degree from the University of Tsukuba, Japan, in 2007. He is currently a Research Assistant at the Global COE Program on ‘Cybernetics: fusion of human, machine, and information systems’, University of Tsukuba, Japan. His research interests include assistive systems for physically challenged persons, biomedical engineering and rehabilitation robotics. He is a Member of the Robotics Society of Japan.



Ryota Kawanishi received the BE degree from the University of Tsukuba, Japan, in 2008. He is currently a Master’s course student of the Department of Information Interaction Technologies, University of Tsukuba, Japan. His research interests include biofeedback training for rehabilitation and human-machine interface.



Yasuhisa Hasegawa received the BE and ME degrees from Nagoya University, Japan, in 1994 and 1996, respectively. From 1996 to 1998, he worked for Mitsubishi Heavy Industries Ltd, Japan. He joined Nagoya University, in 1998, as a Research Associate and received the Dr degree in Engineering from Nagoya University, in 2001. From 2003 to 2004, he was an Assistant Professor at Gifu University. He moved to the University of Tsukuba, in 2004, as an Assistant Professor. He is currently an Associate Professor of the Department of Information Interaction Technologies, University of Tsukuba. He is mainly engaged in the research fields of human intention-based physically assistive robots, dynamic motion control and dexterous robotic hands. He is a Member of the IEEE, Japan Society of Mechanical Engineers, Robotics Society of Japan, Society of Instrument and Control Engineers, and Japan Society for Fuzzy Theory and Intelligent Information. He is also an Associate Vice President of Technical Activities for the IEEE Robotics and Automation Society.



Yoshiyuki Sankai received the Dr degree in Engineering from the University of Tsukuba, Japan, in 1987. He was Assistant Professor, Associate Professor and Professor at the Institute of Systems & Engineering at the University of Tsukuba, and a Visiting Professor of Baylor College of Medicine, Houston, TX. Currently, he is a Professor of the Graduate School of Systems & Information Engineering, University of Tsukuba, and President and CEO of Cyberdyne Inc. He was/is also President of the Japan Society of Embolus Detection & Treatment, Chairman of the International Journal of the Robotics Society of Japan (RSJ), and Executive Board Member of the RSJ. He is the inventor, creator and driving force behind the advanced robotics, Robot Suit HAL[®] (Hybrid Assistive Limb[®]), and various cybernics, medical, care and welfare technologies. In 2006 and 2009, he was invited to provide direction to Japan's future science and technology policies by the Council for Science and Technology Policy advising the Prime Minister, other Japanese ministers and senior government officials. Among the awards he has won are: World Technology Award (2005), Good Design Gold Award (2006), Japan Innovator Award (2006), Best Paper Award (International Journal of Advanced Robotics) (2006), Award from the American Society for Artificial Organs, Award from the International Society for Artificial Organs, Award from the Minister of Economy, Trade and Industry of Japan (2007), Award from the National Institute of Science and Technology Policy (2007), NIKKEI Top-Quality/Service Award (2008), Award from the IEEE/IR, Invention & Entrepreneurship Award (2009), the 21st Century Invention Award from the Japan Institute of Invention and Innovation (2009), etc. He has been selected as the Core Researcher of the Funding Program for World-Leading Innovative R&D on Science and Technology, set up by the Cabinet Office of Japan. He continues to promote the application of the HAL technology for the benefit of senior citizens, physically challenged people and patient groups with specific diseases.